



Comparative Prediction of Epileptic Seizures Based on Phase Synchronization in EEG

S. H. Shokouh-Alaei ^{1,*}, M. A. Khalilzadeh ¹

¹ Faculty of Engineering, Islamic Azad University, Mashhad branch, Mashhad, Iran

ARTICLE INFO	ABSTRACT
<p>Article History: Received 20 June 2019 Received in revised form 29 July 2019 Accepted 23 December 2019 Available online 24 December 2019</p>	<p>Epileptic seizure prediction has garnered significant attention in recent years due to its potential to improve patient outcomes and reduce the burden of epilepsy. The integration of advanced machine learning techniques, particularly deep learning, into seizure prediction models has opened new avenues for research. Currently, epilepsy patients who have not achieved complete seizure control face the challenge of sudden and unpredictable epileptic seizures. A method capable of predicting seizure onset could significantly enhance the quality of life for these individuals. The fundamental basis of seizure prediction lies in distinguishing the preictal phase dynamics from other phases. In this study, phase synchronization is employed as an indicator for analyzing interactions between different brain regions and as a reliable metric for identifying the preictal period. Furthermore, seizure prediction horizon and seizure onset time are two critical factors in evaluating seizure prediction methods. Although previous studies have primarily used these temporal parameters for assessment, this paper incorporates them into a neuro-fuzzy model, allowing for adaptive seizure prediction based on patient feedback. The implementation of the proposed model on intracranial EEG signals demonstrated that, across various time window values, sensitivity and specificity exceeded 70%.</p>
<p>Keywords: Spatiotemporal Frequency Pattern, Adaptive Seizure Prediction, SOP And SPH Analysis, Neuro-Fuzzy Model, Phase Synchronization Index.</p>	

1. INTRODUCTION

Epilepsy is one of the most common neurological disorders, affecting approximately 1% of the global population [1]. This condition arises from excessive, abnormal, and spontaneous electrical discharges in the cerebral cortex, placing a significant proportion of epilepsy patients at risk of severe injury or even death. Currently, patients who have not achieved full seizure control face the challenge of sudden and unpredictable epileptic seizures. Beyond the serious risks associated with surgical intervention, many of these patients experience a profound sense of helplessness, which significantly impacts their quality of life. A method capable of predicting seizure onset could substantially enhance treatment options and, consequently, improve the quality of life for individuals with epilepsy [2].

* Corresponding Author: hesamshokouhalaie@gmail.com
Faculty of Engineering, Islamic Azad University, Mashhad branch, Mashhad, Iran



The fundamental premise of seizure prediction is the identification of a preictal phase. Significant changes in EEG dynamics have been reported within a time window ranging from a few seconds to several hours before seizure onset [3]. The most common approach for distinguishing the preictal phase from the interictal period involves the extraction of linear or nonlinear features from EEG signals. Since the objective is to predict an impending seizure rather than merely detecting its occurrence, the ictal and postictal phases are typically disregarded [4]. The emergence of nonlinear mathematical and physical system theories has introduced novel methods aimed at better characterizing system dynamics compared to linear approaches. However, a common limitation across these studies is their exclusive focus on distinguishing the preictal phase from the ictal phase, without assessing the interictal period. Additionally, the omission of statistical feature characteristics renders these studies incomplete in terms of providing a comprehensive evaluation for reliable seizure prediction [2].

With the advent of high-capacity memory storage, epilepsy monitoring centers have become capable of recording extensive datasets for pre-surgical monitoring. These centers aim to test and compare proposed methods using standardized datasets. Most studies in this domain have demonstrated the weak performance of univariate analysis-based methods, whereas multivariate analysis approaches have yielded better results [2]. Multivariate time-series analysis involves the simultaneous recording of multiple observations over time to examine interactions between different components of a system [5]. Research has shown that, when distinguishing preictal from interictal (non-epileptic) features, nonlinear classifiers outperform linear classifiers in terms of prediction accuracy. Furthermore, among nonlinear classifiers, those capable of adapting to the chaotic and stochastic nature of EEG signals achieved higher prediction accuracy. Consequently, given the online adaptability of predictive models, these classifiers are more practical for real-world applications [6-13].

In this study, long-term EEG data are utilized to quantify the interactions between different brain regions within specific frequency bands using the phase synchronization index. The extracted features are then classified into epileptic and non-epileptic categories in real time using the Gath-Geva neuro-fuzzy model. A methodology similar to [14] is employed for result evaluation, wherein the prediction algorithm is trained based on two temporal indices, Seizure Onset Prediction (SOP) and Seizure Prediction Horizon (SPH), which are used for performance assessment. It is expected that the proposed approach will yield satisfactory results across various temporal parameters.

The remainder of this paper is structured as follows: Section 2 introduces the dataset and details the preprocessing steps. Section 3 describes the proposed methodology, including EEG frequency band decomposition, phase synchronization index extraction, optimal feature selection, final feature classification, adaptive seizure prediction, and evaluation methods. Section 4 presents the implementation results and performance analysis, while Section 5 discusses the conclusions and final remarks.

2. DATA AND PREPROCESSING

This study utilizes data from the Freiburg Epilepsy Database. This database contains invasive EEG recordings from 21 patients with focal epilepsy. The recorded EEG data for each patient includes both epileptic and interictal samples. Specifically, the epileptic dataset consists of 50 minutes of EEG data preceding seizure onset, while the interictal dataset contains 24 hours of normal, non-epileptic EEG data. For each patient, six recording channels were selected: three electrodes positioned near the epileptic focus and three channels located outside the seizure focus [15].

For analyzing the recorded data, a moving window approach is employed. Each processing window consists of 4,096 samples, corresponding to 16 seconds, with a 20% overlap between consecutive windows. After segmenting the EEG data into windows, preprocessing is performed using an 18th-order finite impulse response (FIR) low-pass filter with a cutoff frequency of 70 Hz to eliminate high-frequency noise. Additionally, an infinite impulse response (IIR) notch filter with a cutoff range of 49–51 Hz and a 16th-order design is applied to remove power line interference.

3. PROCESSING, CLASSIFICATION, AND EVALUATION

3.1. EEG Frequency Band Decomposition

To compute the phase synchronization index, it is necessary to extract the instantaneous phase of the signal using the Hilbert transform. Since recent applications of the Hilbert transform are primarily restricted to narrowband signals, the EEG signal is decomposed into frequency bands (delta, theta, alpha, beta, and gamma) using Hilbert-Huang Transform (HHT) analysis. The steps of this technique are summarized as follows [16]:

1. The EEG signal is decomposed into intrinsic mode functions (IMFs) using the empirical mode decomposition (EMD) algorithm.
2. By applying the Hilbert transform to each IMF, the frequency content of each time sample is obtained.

Since the original signal is reconstructed by summing the IMFs for each time sample, individual frequency bands can be extracted. For instance, to obtain the beta band, IMFs with frequency content ranging from 12 to 30 Hz are selected for each sample. The selected IMFs are then summed to reconstruct the beta-band signal. This process is repeated for the other frequency bands.

3.2. Phase Synchronization Index

To apply the phase synchronization index, it is necessary to extract the phase components of two signals from their respective time series. The Hilbert transform is a widely used technique for extracting the instantaneous phase. Considering an analytic signal $z(t)$ as defined in Equation (1), the Hilbert transform ensures that the real part of the analytic signal, $x(t)$, corresponds to the imaginary part of the analytic signal, $\hat{y}(t)$.

At this stage, after decomposing the EEG into frequency bands, the processing steps for each frequency band continue following the approach in [17]. Initially, the DC component of the signal is removed within each window. To mitigate edge effects, a Hamming window is then applied to the segmented signal. Subsequently, to address the discrepancy between the finite length of the data and Equation (2), the Hilbert transform is applied to the signal. After obtaining the instantaneous phase according to Equation (3), 10% of the computed phase values from both ends of the signal are discarded to minimize boundary effects.

$$z(t) = x(t) + i\hat{y}(t) = A(t)e^{i\theta(t)} \tag{1}$$

$$H[x(t)] \equiv \hat{y}(t) = \frac{1}{\pi} PV \int_{-\infty}^{\infty} \frac{x(\tau)}{t-\tau} d\tau \tag{2}$$

$$\theta(t) = \tan^{-1}\left(\frac{\hat{y}}{x}\right) \tag{3}$$

One of the multivariate analysis techniques involves utilizing the concept of phase synchronization [18]. In this approach, the set of instantaneous phases obtained in the previous step is stored in an index vector φ for each time window. Before computing the phase synchronization index for two oscillatory systems (i.e., two recorded channels), it is necessary to determine the phase difference between the two systems using Equation (4).

$$\varphi_{n,m}^{12}(t) = |n\varphi_1(t) - m\varphi_2(t)| = const. \tag{4}$$

The integers n and m specify the frequency locking ratio, indicating at which multiples of the phase components the synchronization between the two oscillatory systems occurs. The term $\varphi_{n,m}^{12}(t)$ represents the generalized phase difference or the relative phase between systems 1 and 2. In this measure, no constraints are imposed on the signal amplitudes. In other words, phase synchronization between two coupled systems implies a relationship between their phase components, while their respective amplitudes may remain uncorrelated [18], [17].

To quantitatively assess the degree of synchronization, the mean phase coherence measure [19], based on the conditional probability index, is employed. Accordingly, the mean phase coherence for N observed samples from two oscillatory systems (1 and 2) with a frequency ratio of $n:m=1:1$ and a sampling rate of $\frac{1}{\Delta t}$ is defined using the relative phase values obtained from Equation (4), as formulated in Equation (5).

$$R_{1,2} = \left| \frac{1}{N} \sum_{j=0}^{N-1} e^{-j\varphi_{1,1}^{12}(j\Delta t)} \right| \tag{5}$$

In this study, instead of computing $R_{1,2}$ for two EEG channels, we calculate the phase coherence index for the delta frequency band between EEG channels 1 and 2, denoted as $R_{1,2}^\delta$. The same measure is then determined for the other frequency bands (theta, alpha, beta, and gamma) between channels 1 and 2.

Furthermore, in general, there exist $M \times (M-1)/2$ unique, non-redundant EEG channel pairs. For instance, in this study, where six channels are used to record signals for each individual, a total of 15 possible channel pairings are available for computing features in each frequency band. Consequently, by considering the phase synchronization index for each distinct channel pair, a set of indices can be stored in a matrix (6), which defines the spatial-frequency pattern for each individual.

$$Features = \begin{bmatrix} R_{1,2}^\delta, R_{1,2}^\theta, R_{1,2}^\alpha, R_{1,2}^\beta, R_{1,2}^\gamma \\ R_{1,3}^\delta, R_{1,3}^\theta, R_{1,3}^\alpha, R_{1,3}^\beta, R_{1,3}^\gamma \\ \vdots \\ R_{5,6}^\delta, R_{5,6}^\theta, R_{5,6}^\alpha, R_{5,6}^\beta, R_{5,6}^\gamma \end{bmatrix}_{15 \times 5} \tag{6}$$

3.3. Optimal Feature Selection

It is well understood that an excessive number of indices increases computational complexity and significantly raises the likelihood of false alarms. Conversely, it can be asserted that major dynamic changes, arising from the interactions of different brain regions, consistently manifest in specific oscillators or, more precisely, in particular brain regions before the onset of a seizure. This observation suggests that only certain indices effectively reflect the dynamic changes associated with epileptic seizures.

Therefore, it is crucial to select a subset of the 75 features that enables highly accurate seizure prediction. To achieve this, we first evaluate the strength of the relationship between epileptic and non-epileptic indices using the Spearman correlation coefficient statistical test. Subsequently, indices exhibiting minimal correlation with one another (i.e., those with near-zero correlation coefficients or statistically significant differences between the two groups) are selected as optimal indices [20].

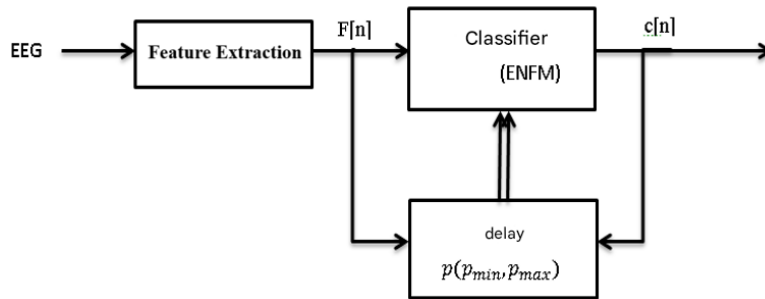


Fig. 1. Block Diagram of the Proposed Model Training

3.4. Classification of Extracted Features and Adaptive Prediction of Seizure Attacks

In this study, a fuzzy clustering-based classifier is used. A common issue with fuzzy clustering algorithms is their limitation in offline applications. Therefore, using offline-mode algorithms with long-term data leads to increased computational complexity and significant time consumption. Additionally, in practical applications, predictive models must adapt over time to track changes in system behavior. To address this, we propose a fuzzy recursive clustering-based neural-fuzzy model for distinguishing epileptic from non-epileptic features [6].

Due to the advantages of Gath-Geva clustering over K-means clustering in terms of its ability to form different shapes of clusters, and its superiority over Gustafson-Kessel clustering in producing clusters of varying sizes, Gath-Geva clustering is used as the basis for the fuzzy recursive clustering algorithm [6].

The basis for prediction is to continuously alert the patient within a time frame before the onset of a seizure. The length of this time frame is equal to the seizure prediction time (p). In seizure prediction, an ideal warning system should differentiate the pre-seizure period from the seizure and normal periods. As shown in Figure 1, if the extracted features in each time window are denoted as $f[n]$, the model output $c[n]$ will be either +1 or -1, depending on whether the patient is in a pre-seizure or non-seizure state. In online models, due to the causal nature of the system, all non-seizure windows are labeled as -1, and the labeling of the pre-seizure period is determined through feedback from the patient at the moment the attack begins. Therefore, when the patient experiences a seizure, at the moment the seizure begins, an indicator for the attack's occurrence must be triggered. Then, based on the two time features specified in the evaluation method of this paper, all windows from $p_{max} - p_{min}$ before p_{min} up to the start of the attack are labeled as +1.

It is important to note that in online training algorithms, there is a delay of p_{max} between the training and testing samples. In the case of the ENFM classifier, at the n th moment, the model is trained based on the input $f[n - p_{max}]$ and the output $c[n - p_{max}]$. Using the trained model, for each input $f[n]$, an output $c[n]$ is obtained. The method for selecting p_{max} and p_{min} is explained in the following section.

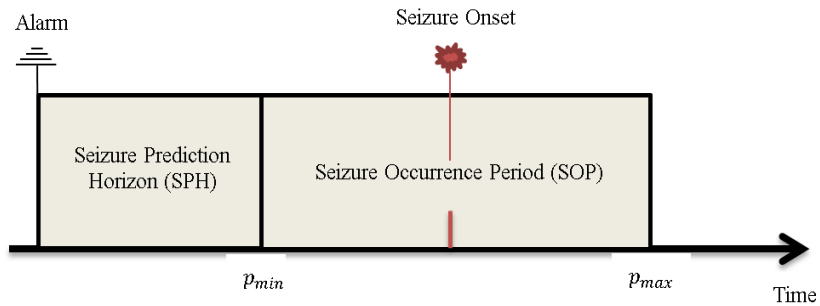


Fig. 2. Concept of SOP and SPH Intervals

3.5. Seizure Prediction Evaluation

An ideal prediction approach would be able to pinpoint the exact moment of a seizure; however, such ideal behavior is not expected from current prediction methods. This uncertainty in determining the exact time of the attack is expressed by defining an interval in which the seizure is expected to occur (seizure occurrence period or SOP) (Figure 2) [14]. Additionally, in order for preventive measures (such as medication, electrical stimulation, or simply issuing alerts to avoid dangerous situations) to be applied effectively, the period between the warning and the beginning of the SOP is crucial (seizure prediction warning or SPH). It is expected that no attack occurs during this interval.

A noteworthy point is that during the training process of the neural-fuzzy model, the delay time p is determined based on the SOP and SPH time intervals. Specifically, the time interval in which the model output is labeled as +1 after detecting the attack corresponds to the SOP interval ($p_{max} - p_{min}$), and the duration from the end of this interval to the onset of the attack is equivalent to the SPH duration (p_{min}). Therefore, it is expected that the predictive system is properly trained for each SOP and SPH defined.

The performance of the seizure prediction algorithm is evaluated using statistical metrics such as sensitivity and specificity (7), (8), which are detailed below:

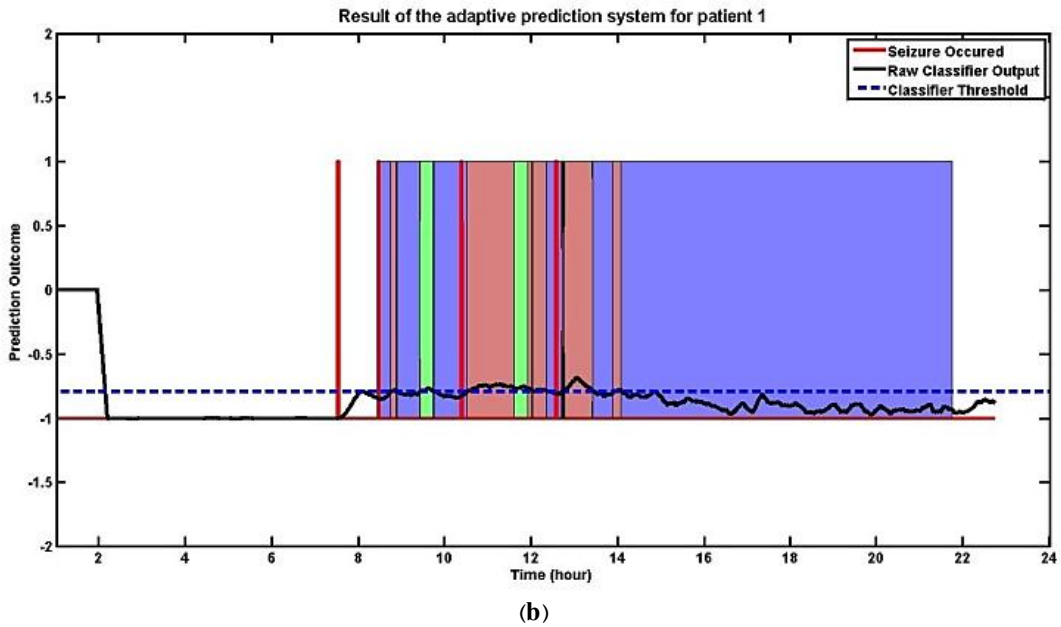
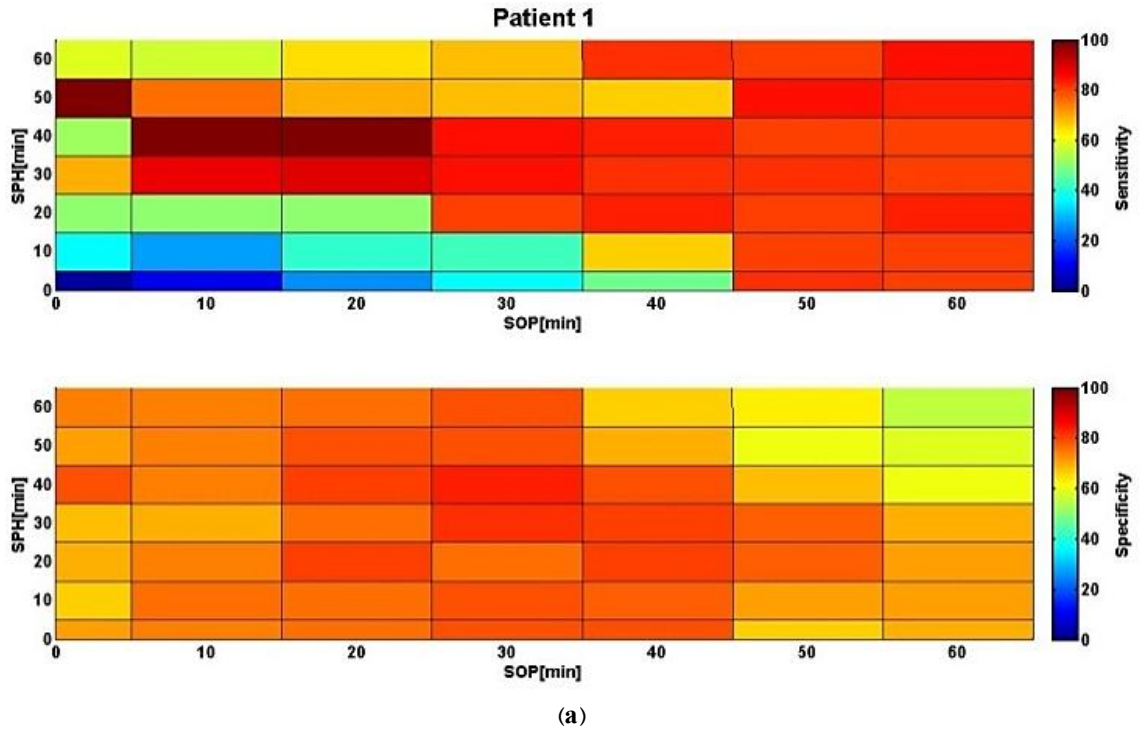


Fig. 3. Results for Patient 1, (a) Sensitivity and specificity for different SOP and SPH values (b) Model output for SOP=20 and SPH=40 (Sensitivity: 98.9%, Specificity: 80.04%)

$$Sensitivity = \frac{TP}{TP+FN} \tag{7}$$

$$Specificity = \frac{TN}{TN+FP} \tag{8}$$

Output Prediction Categories Based on SOP and SPH

Given the previously defined SOP and SPH ranges, the prediction output can be categorized into one of the following four outcomes:

If $c[n] = 1$ and at least one seizure occurs within the SOP range after SPH, then it is a true positive result.

If $c[n] = 1$ and no seizure occurs within the SOP range after SPH, then it is a false positive result.

If $c[n] = 0$ and no seizure occurs within the SOP range after SPH, then it is a true negative result.

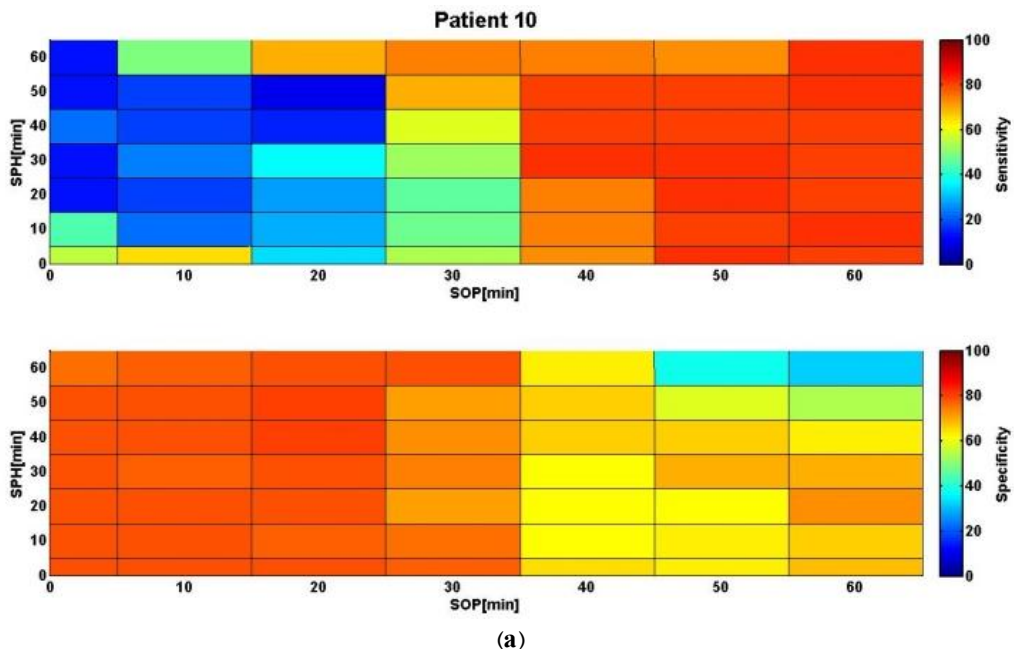
If $c[n] = 0$ and at least one seizure occurs within the SOP range after SPH, then it is a false negative result.

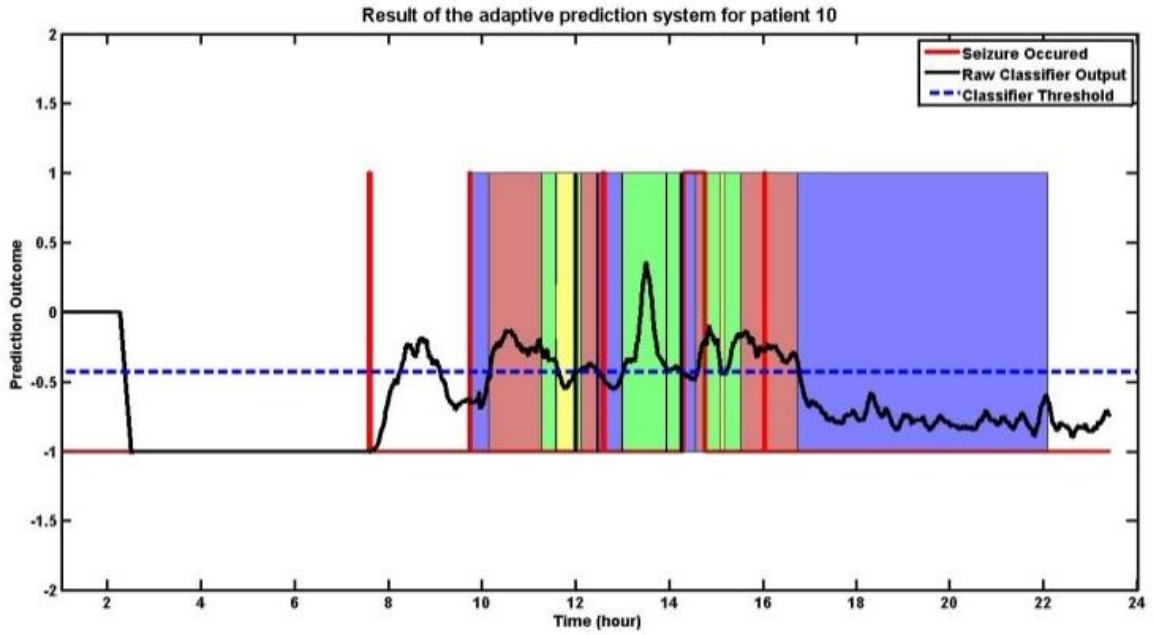
4. IMPLEMENTATION AND RESULTS ANALYSIS

The results of the proposed model are presented for four epileptic patients in this study. Given the online nature of this model and the need for a correct evaluation of the prediction performance, approximately 5 hours of non-epileptic EEG data were added at the beginning of each seizure event, and the evaluation is only performed after the second seizure event. Therefore, evaluation takes place after the second seizure until the end of the data collection period.

In this study, the output of the fuzzy-neural classifier (ENFM) was compared with a threshold, and if the value exceeds the threshold, an impending seizure warning is issued. In an automatic feedback system, this threshold is adjusted to achieve sensitivity and specificity values above 80%, if possible.

To achieve optimal performance, the sensitivity and specificity results of the proposed model were obtained for various SOP and SPH values: 60, 50, 40, 30, 20, 10, and 5 minutes, as shown in Figures (3), (4), and (5). As shown in Figure (3-a), Patient 1 achieved good results for medium SOP and SPH values, with sensitivity of 98.94% and specificity of 80.04% for an SOP of 20 minutes and SPH of 40 minutes. The model output for these values is shown in Figure (3-b), where seizure events are marked with vertical red lines, and true positive, false positive, true negative, and false negative results are marked in green, red, blue, and yellow, respectively.





(b)

Fig. 4. Results for Patient 10

(a) Sensitivity and specificity for different SOP and SPH values. •

(b) Model output for SOP = 60 minutes and SPH = 20 minutes (Sensitivity: 81.61%, Specificity: 69.75%). •



(a)

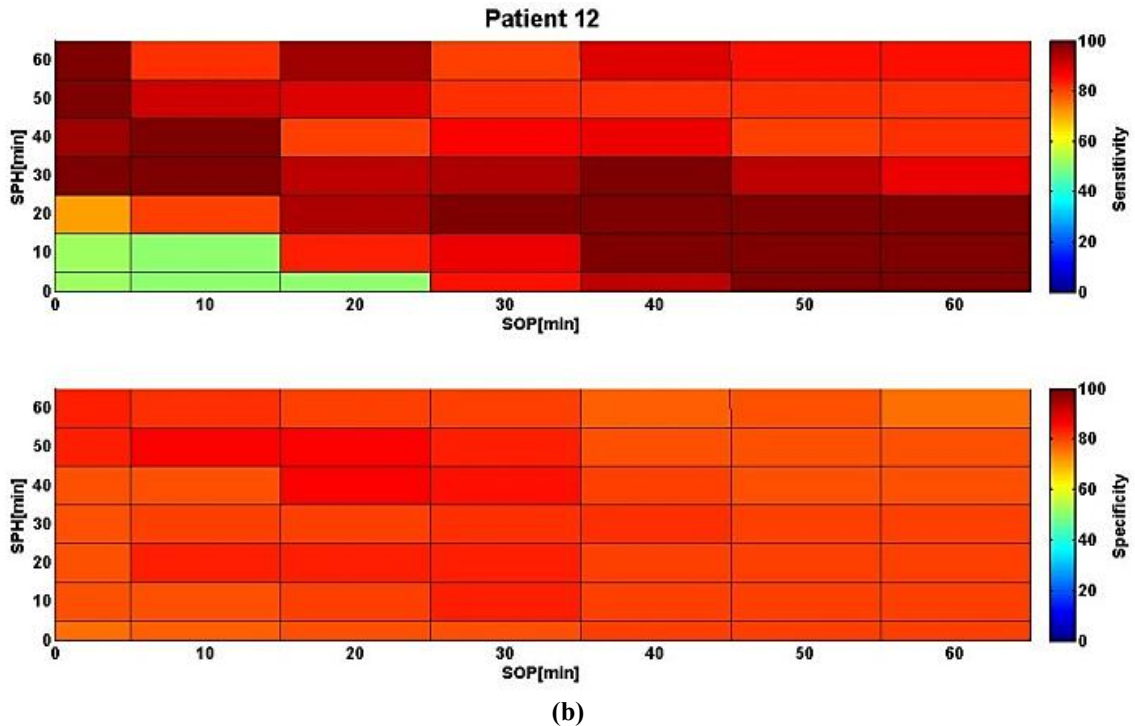


Fig. 5. Sensitivity and Specificity Results for Patients 2 and 12 for Different SOP and SPH Values

In the analysis of Figure 4-a and Figure 5, the following trends were observed:

Patient 2 performed well with higher SOP and lower SPH, or vice versa (low SOP and high SPH), yielding acceptable results.

For Patient 10, the best performance was observed with SOP = 60 and SPH = 20 (Figure 4-b).

For Patient 12, excellent results were obtained for most SOP and SPH values, except for those with low SOP and low SPH.

Overall results across the 4 patients showed that under optimal conditions (best SOP and SPH), the average sensitivity reached 89.89% and specificity reached 81.18%.

5. DISCUSSION AND CONCLUSION

This research utilized the phase synchrony index between pairs of EEG channels across different frequency bands to capture brain region interactions. By employing this index, a neuro-fuzzy model was developed to predict seizures adaptively based on the attack occurrence window and prediction window. The results indicated that for most SOP and SPH values, statistical features of sensitivity and specificity exceeded 70%.

The analysis also highlighted that increasing the prediction window duration could be more beneficial for subjects in preventing the consequences of an attack. On the other hand, reducing the attack occurrence window helps in reducing patient stress and anticipation.

In future research, it's suggested to design an algorithm for determining the optimal SOP and SPH values to further enhance the performance of the proposed model and improve the prediction system.

Transparency Statement

The data supporting this study are available upon reasonable request to the corresponding author, subject to ethical and confidentiality considerations.

Acknowledgments

We would like to express our gratitude to all individuals who contributed to this project.

Declaration of Interest

The authors declare that they have no competing interests.

Funding

This research received no specific grant from any funding agency, commercial, or not-for-profit sectors.

REFERENCES

- [1] Litt, B., & Lehnertz, K. (2002). Seizure prediction and the pre-seizure period. *Current Opinion in Neurology*, 15(2), 173–177. <https://doi.org/10.1097/00019052-200204000-00008>
- [2] Mormann, F., Andrzejak, R. G., Elger, C. E., & Lehnertz, K. (2007). Seizure prediction: The long and winding road. *Brain*, 130(2), 314–333. <https://doi.org/10.1093/brain/awl241>
- [3] Schelter, B., Winterhalder, M., Maiwald, T., Brandt, A., Schad, A., Timmer, J., & Schulze-Bonhage, A. (2006). Do false predictions of seizures depend on the state of vigilance? A report from two seizure-prediction methods and proposed remedies. *Epilepsia*, 47(12), 2058–2070. <https://doi.org/10.1111/j.1528-1167.2006.00848.x>
- [4] Mirowski, P., et al. (2009). Classification of patterns of EEG synchronization for seizure prediction. *Clinical Neurophysiology*, 120(11), 1927–1940. <https://doi.org/10.1016/j.clinph.2009.09.002>
- [5] Carney, P. R., et al. (2011). Seizure prediction: Methods. *Epilepsy & Behavior*, 22(Suppl. 1), S94–S101. <https://doi.org/10.1016/j.yebeh.2011.09.001>
- [6] Soleimani-B, H., et al. (2012). Adaptive prediction of epileptic seizures from intracranial recordings. *Biomedical Signal Processing and Control*, 7(5), 456–464. <https://doi.org/10.1016/j.bspc.2011.11.007>
- [7] Maniyath, S. R., Vinod, V. P., Niveditha, M., Pooja, R., Bhat, N. P., Shashank, N., & Hebbar, R. (2018). Plant disease detection using machine learning. In *2018 International Conference on Design Innovations for 3Cs Compute Communicate Control (ICDI3C)* (pp. 41–45). <https://doi.org/10.1109/ICDI3C.2018.00017>
- [8] Crawford, M., Khoshgoftaar, T., Prusa, J. D., Richter, A. N., & Najada, H. A. (2015). Survey of review spam detection using machine learning techniques. *Journal of Big Data*, 2, 1–24. <https://doi.org/10.1186/s40537-015-0029-9>
- [9] Wang, L., Xue, W., Li, Y., Luo, M.-L., Huang, J., Cui, W., & Huang, C. (2017). Automatic epileptic seizure detection in EEG signals using multi-domain feature extraction and nonlinear analysis. *Entropy*, 19(6), 222. <https://doi.org/10.3390/e19060222>
- [10] Meidan, Y., Bohadana, M., Mathov, Y., Mirsky, Y., Breitenbacher, D., & Elovici, Y. (2017). Detection of unauthorized IoT devices using machine learning techniques. *arXiv preprint, arXiv:1709.04647*.
- [11] Sultana, N., Chilamkurti, N., Peng, W., & Alhadad, R. (2018). Survey on SDN based network intrusion detection system using machine learning approaches. *Peer-to-Peer Networking and Applications*, 12, 493–501. <https://doi.org/10.1007/s12083-017-0630-0>
- [12] Islam, M. R., Kabir, M. A., Ahmed, A., Kamal, A., Wang, H., & Ulhaq, A. (2018). Depression detection from

social network data using machine learning techniques. *Health Information Science and Systems*, 6. <https://doi.org/10.1007/s13755-018-0046-0>

- [13] Mullen, T., Kothe, C., Chi, Y., Ojeda, A., Kerth, T., Makeig, S., Jung, T., & Cauwenberghs, G. (2015). Real-time neuroimaging and cognitive monitoring using wearable dry EEG. *IEEE Transactions on Biomedical Engineering*, 62, 2553–2567. <https://doi.org/10.1109/TBME.2015.2481482>
- [14] Schelter, B., Winterhalder, M., Maiwald, T., Brandt, A., Schad, A., Schulze-Bonhage, A., & Timmer, J. (2006). Testing statistical significance of multivariate time series methods for epileptic seizure prediction. *Chaos*, 16(1), 013108. <https://doi.org/10.1063/1.2137623>
- [15] Ihle, M., Feldwisch-Drentrup, H., Teixeira, C. A., Witon, A., Schelter, B., Timmer, J., & Schulze-Bonhage, A. (2012). EPILEPSIAE: A European epilepsy database. *Computer Methods and Programs in Biomedicine*, 106(3), 127–138. <https://doi.org/10.1016/j.cmpb.2010.08.011>
- [16] Huang, N. E., Shen, Z., Long, S. R., Wu, M. C., Shih, H. H., Zheng, Q., Yen, N. C., Tung, C. C., & Liu, H. H. (1998). The empirical mode decomposition and the Hilbert spectrum for nonlinear and non-stationary time series analysis. *Proceedings of the Royal Society of London. Series A: Mathematical, Physical and Engineering Sciences*, 454, 903–995. <https://doi.org/10.1098/rspa.1998.0193>
- [17] Nasiri, S., & Sharafat, A. (2010). Prediction of epileptic seizures using phase synchronization analysis in time-frequency domain. *Proceedings of the 19th Iranian Conference on Electrical Engineering*, Amirkabir University of Technology, Tehran, Iran, 6.
- [18] Rosenblum, M., et al. (2001). Chapter 9: Phase synchronization: From theory to data analysis. In *Handbook of Biological Physics*. [https://doi.org/10.1016/S1383-8121\(01\)80012-9](https://doi.org/10.1016/S1383-8121(01)80012-9)
- [19] Mormann, F., et al. (2000). Mean phase coherence as a measure for phase synchronization and its application to the EEG of epilepsy patients. *Physica D: Nonlinear Phenomena*, 144(3), 358–369. [https://doi.org/10.1016/S0167-2789\(00\)00087-7](https://doi.org/10.1016/S0167-2789(00)00087-7)
- [20] Daniel, W. W. (1990). Spearman rank correlation coefficient. In *Applied Nonparametric Statistics* (2nd ed., pp. 358–365). Boston: PWS-Kent. ISBN 0-534-91976-6.